Journal of Nanoporous Systems

Original Research Paper

Removal of pharmaceutical pollutant cefixime from aqueous solutions using SBA-16 mesostructure modified with NH_2 group and optimization of effective parameters by experiment design software

Samaneh Soleymani[1, *] | Maryam Razavi Mehr[2] | Fatemeh Saki[1]

[1]*Department of Chemistry, Faculty of Chemistry, Lorestan University, Khorramabad, Iran*
[2]*Department of Education, Faculty of Teacher Education, Farhangian University, Boroujerd, Iran*

Article history
Received: 23 December 2024
Revised: 16 March 2025
Accepted: 14 April 2025

*Corresponding Author,
Email:
Samanesoleymani1988@gmail.com

Abstract: In this research, the mesostructure of SBA-16 was synthesized and its surface was modified by NH_2 group to increase efficiency. And then the prepared SBA-16-NH_2 was used as an adsorbent to remove the pharmaceutical pollutant cefixime from aqueous environments. The mesoporous structure of SBA-16-NH_2 was analyzed by Fourier transform infrared spectroscopy (FTIR), X-ray diffraction (XRD), Thermogravimetric analysis (TGA), scanning electron microscopy (SEM) and transmission electron microscopy (TEM). Then, the effect of different parameters such as pH, initial concentration of cefixime, amount of SBA-16-NH_2 adsorbent, temperature and contact time on the absorption of medicinal pollutant cefixime by the prepared adsorbent was investigated with the help of experiment design software. The results of the predicted experiments showed that the highest absorption of cefixime is seen at pH=4, temperature 43°C, contact time 35 min., initial adsorbent concentration 10 ppm and adsorbent amount 0.049 g. In optimal conditions, SBA-16-NH_2 adsorbent could remove 98.88% of cefixime from aqueous medium. Also, Langmuir, Freundlich and Temkin isotherms were investigated and the results indicated that the adsorption behavior is mostmostly consistent with Langmuir isotherm. The results of thermodynamic experiments also indicated that the absorption process is exothermic and spontaneous.

Keywords: Nanomesoporous SBA-16-NH_2, Pharmaceutical pollutants, Antibiotic, Cefixime, Experimental design, Response surface method.

Introduction

Increasing living standards and changing production and consumption patterns lead to the emergence of new materials. Drugs are widely used for the prevention and treatment of diseases in humans and as veterinary drugs [1]. These biologically active chemicals are considered emerging pollutants due to their persistence and potential harmful effects on aquatic ecosystems. These emerging pollutants, which continuously enter the aquatic environment at low concentrations, remain active even at low concentrations and deteriorate water quality and adversely affect ecosystems and human health. In the meantime, the high consumption of drugs leads to the simultaneous concern of observing its presence in the environment, because a large amount of these therapeutic compounds cannot be absorbed and metabolized by the human body, so they are excreted through feces and urine and enter the wastewater treatment plant (WWTP) [2,3]. The main ingredients of pharmaceutical waste are antibiotics, chemotherapy products, hormones, painkillers, antipyretics and antidepressants. Many studies have shown that various drugs are present in aquatic environments. The environmental concentration of antibiotics, antidepressants, chemotherapy products, analgesic compounds, hormones and lipid regulators varies from 0.04 to 6.3 µg/L. The primary sources of pharmaceutical pollutants in the environment are pharmaceutical industries, hospitals, animal excreta, research activities using therapeutic compounds, and discharge of expired drugs in the environment. Among the various sources, hospitals have a major contribution

to the release of drugs into the environment. Amount of water consumption in hospitals is between 400 and 1200 liters per day [4]. Effluent from hospitals contains pathogens, drug residues and their metabolites, drug compounds, radioactive elements and other chemicals. Discharge of hospital wastewater to urban WWTP (even at diluted medicinal concentrations) reduces the biodegradation process of organic pollutant in WWTP. The direct discharge of treated effluent (containing pharmaceuticals) from WWTPs into natural water bodies raises concerns about the impact of these persistent compounds on aquatic ecosystems. The presence of these medicinal pollutants in the receiving environment causes disturbances in aquatic animals and endangers human health. Many short-term toxicity studies reported that drug molecules do not have an acute toxic effect on aquatic organisms due to their presence in low concentration, but their continuous release and exposure to aquatic organisms have long-term (chronic) effects [5-7]. Long-term exposure to drugs in low concentration leads to changes in species and behavior of aquatic organisms. Exposure to dutasteride reduces fish fertility and also affects the reproductive performance of male and female fish. Medicines usually have a bioactive, resistant and cumulative nature. These features are the main causes of harmful effects such as endocrine disorders, reproductive abnormalities, bacterial resistance, environmental toxicity even at low concentrations. According to the World Health Organization, these pollutants usually enter the wastewater through the disposal of unmetabolized compounds after medical use and misuse, whose metabolites can be much more harmful than the original compound itself [8].

Antibiotics are one of the most widely used drug groups in medicine and veterinary medicine. These drugs fall into several categories, such as quinolones (and fluoroquinolones), tetracyclines, macrolides, sulfonamides, and beta-lactams. Fluoroquinolones, macrolides and aminoglycosides are divided. Most of the antibiotics are prescribed in human medicine, while penicillins, tetracyclines and macrolides are the most prescribed antibiotics in veterinary medicine [9]. So far, nearly 250 antibiotics have been registered in human and veterinary medicine. The origin of antibiotics can be natural (usually products of secondary metabolism of fungi or bacteria), semi-synthetic (by-products derived from natural products), or synthetic. Since the last decade, the global consumption and use of antibiotics increased by more than 30%, from approximately 50 to 70 billion standard units (SU). Antibiotics are often considered as pseudo-persistent compounds because they are continuously introduced into the environment. The emergence and release of antibiotics are particularly concerned because they are designed to kill and inhibit the growth of microorganisms, thus, inhibiting the activity of beneficial microbes in WWTP operations and in their removal. Furthermore, due to the continuous exposure to antibiotics, the microbial community residents in wastewater develop more resistant mechanisms than the rest of the microbial world [10,11]. The presence of multiple antibiotic compounds in untreated wastewater was observed in aqueous and solid phase. Sulfonamides, macrolides, and fluoroquinolone antibiotics are commonly found and persist in surface water and wastewater. In general, the presence and persistence of antibiotics in water can be seen as a concern, as approximately 90% of antibiotics consumed by the human body are excreted through urine and feces. Cefixime (Fig 1), was discovered in 1979 and was approved for medical use in the United States in 1989. There are three water molecules in the structure of this drug, which is called cefixime trihydrate, and due to the presence of the NH group of cefixime trihydrate, it has a high ability to oxidize. Cefixime is a type of antibiotic that belongs to the family of cephalosporin antibiotics and is effective in the treatment of various microbial infections. This medicine is prescribed for the short-term treatment of infections, including urinary tract infection, chest infection, ear infection, and throat infection [12]. Cefixime is effective in treating various microbial infections and has no effect on viral infections such as colds and flu. This drug destroys bacteria by inhibiting the construction of their cell wall [13,14].

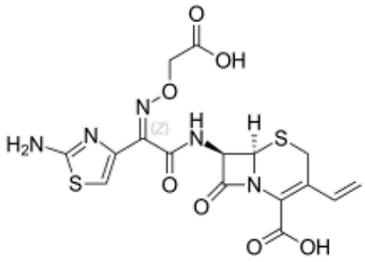

Fig 1. Chemical structure of the antibiotic cefixime

In recent years, special attention has been paid to emergency pollutants including pharmaceutical compounds such as antibiotics in the environment and especially in water sources. Toxicity, carcinogenicity, mutagenesis and damage to DNA, non-biodegradability and drug resistance in antibiotics have caused these compounds to be called pseudo-persistent pollutants in the environment. As a result, the removal of pharmaceutical pollutants has attracted a lot of attention [15]. Among the methods that are used today to remove pollutants, we can mention biological, chemical, and combination of chemical, biological, and physical methods. The process of adsorption, including physical methods, has received more attention compared to other treatment techniques in terms of

initial cost, reuse of wastewater, simplicity and flexibility in design, easy operation, and insensitivity to pollutants and toxic compounds. The production of high-quality wastewater and the absence of free radicals and dangerous substances are among the other advantages of this method [16].

Porous nanostructures are a special group of materials that have cavities/porosity at the nanoscale and exhibit different physicochemical properties. These properties are determined by their shape, size and composition. Compared to uniform particles of the same size, porous nanomaterials have unique properties due to their empty spaces, such as low density, large active surfaces, low refractive index, favorable permeability, good selectivity, and thermal and acoustic resistance. The above mentioned characteristics of porous nanostructures have led to the presentation of diverse nanoporous materials, which have attracted the attention of scientists in various fields [17]. Among these porous solids, mesopores are more efficient than others due to their large surface area, high porosity, tunable pores, excellent thermal properties, and mechanical stability. Silica-based mesoporous Santa Barbara amorphous (SBA) materials have been widely used as adsorbents. SBA-16, the main subset of these materials, particles containing parallel open mesochannels with a narrow and tunable pore size distribution over a wide range from 6 to 12 nm, high surface area, uniform pore size, high pore volume, thermal and chemical stability, hydrophobicity or controllable hydrophilicity, insolubility in water, non-toxic, significant mechanical resistance and high concentration of active sites on their surfaces, biocompatible and biodegradable, wall thickness of about 3 to 4 nm, and have higher mechanical stability and hydrothermal stability than MCM-41 compounds. Such properties make these materials dominant for absorption [18,19]. However, these meso structures do not have a wide range of functional groups on their surfaces (mainly containing silane groups), which limits the possible applications of these materials for specific target molecules. As a solution, many studies have made modifications to the active sites of SBA-16, adding a variety of ligands (organic groups, coordinating compounds, nanoparticles, etc.) and enabling the loading of various compounds on them [20].

In this study, SBA-16-NH_2 nanosilicate was used as cefixime pharmaceutical pollutant adsorbent due to the simple synthesis process and well-defined morphology, large pore size, and especially the three-dimensional connection of pores that causes better mass transfer. After identification by different techniques (XRD, SEM, TEM, etc.), the prepared adsorbent was used to investigate cefixime pollutant removal studies. Then, with the help of experiment design software, the optimal conditions for cefixime removal by SBA-16-NH_2 adsorbent were obtained. Five effective variables in pollutant removal including pH, contact time, temperature, cefixime initial concentration and adsorbent amount were considered. Adsorption isotherms, thermodynamics and kinetics of adsorption were also studied.

Materials and Methods

Chemicals

Pluronic copolymer F127, 3-aminopropyltrioxysilane (APTEOS) and tetraethyl orthosilicate (TEOS) with a purity of 99.00 % were obtained from Sigma Aldrich Company. Cefixime antibiotic, double distilled water.

Characterization

The Netherlands AXS-D8Advance model device with Cu Kα radiation source with 2θ=0.5-70° was used for X-ray diffraction (XRD) measurement. Morphology studies were performed using scanning microscope (SEM) and transmission microscope (TEM) with HITACHI and S-3400N models from Japan, respectively. The functional groups of the absorbent structure were identified using Fourier transform infrared spectroscopy (FTIR). Spectrophotometric measurements were performed by a UV/Vis spectrophotometer (Dynamica-HALO-DB-20, Germany). BET analysis was performed by nitrogen (N2) adsorption and desorption isotherm at 77 K temperature to investigate surface area, size and pore volume (NanoSORD92 model, Japan). Thermogravimetric analysis (TGA) was performed in a nitrogen environment at a temperature of 1000 degrees Celsius and a speed of 5 revolutions per minute by TA company model Q600 made in America. Also, in this research, pH meter (ST2100, Switzerland), magnetic stirrer (Labinco-L81ST, Netherlands), oven (Memmert, Germany), ultrasonic (Elmasonic-S, Germany) and centrifuge (Teb-X-400 rpm, Iran) were used.

Synthesis of SBA-16-NH_2

In this work, by functionalizing nanosilicate SBA-16 by -NH_2 group, its efficiency was improved. To prepare SBA-16-NH_2, 3 g of F127 copolymer were dissolved in 144 ml of distilled water and 9 ml of hydrochloric acid. The mixture was stirred at 35 ℃ until the surfactant was completely dissolved. Then, 9 ml of 1-butanol alcohol was added to it and stirred for one hour. After that 13.2 g of TEOS and 0.85 ml of 3-aminopropyltrioxysilane were added to the solution. The mixture was stirred for 24 hours at a temperature of 35 ℃ on a magnetic stirrer and placed in an oven at a temperature of 100 ℃ for 24 hours. Finally, the template was removed using ethanol extraction [21].

Cefixime drug calibration curve

Solutions with certain concentrations (10-100 ppm) were prepared from the mother solution with a concentration of 1000 ppm of cefixime and the absorbance of the desired solutions was read by UV-Vis device at the maximum wavelength of cefixime (288 nm). By drawing the absorption-concentration diagram, the best equation of the line to obtain the unknown concentrations was obtained (Fig 2).

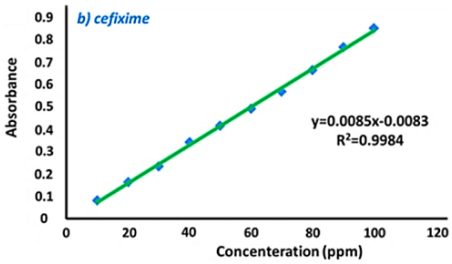

Fig 2. Calibration curve of cefixime drug adsorption

The pH_{PZC} of SBA-16-NH_2

In the process of surface adsorption, at pH_{PZC} the electric charge density on the surface is zero. When the pH of the environment is lower than the pH_{PZC} value, there are more protons on the surface, and the surface of adsorbent becomes positively, which is able to adsorb anions. Conversely, if the pH is higher than pH_{PZC}, the surface becomes negatively charged, which is important in absorbing harmful cations. To determine pH_{PZC}, 0.01 g of SBA-16-NH_2 was dissolved in 15 ml of distilled water. Solutions of SBA-16-NH_2 were prepared and each solution was adjusted to a pH (pH_i= 2-12) by HCl and NaOH. After stirring the solution for 1 hour, the pH was read again (pH_f). By drawing the graph of pH_f *vs.* pH_i (Fig 3), the pH_{PZC} was obtained.

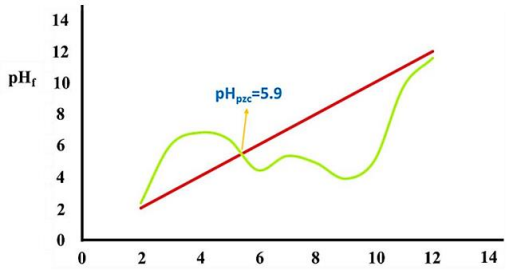

Fig 3. The pH_{PZC} of SBA-16-NH_2 adsorbent

Experiment design using the response surface method

Response surface method (RSM) is a statistical method used in the development of statistical models to solve various equations. This method is based on predicting the functional relationship between the response and the experimental variables [22]. It also optimizes variables. The response surface method uses a series of designed experiments and obtains an optimal response for the entire method that is dependent on the process variables. Central composite design or CCD is the most common method used at the time of optimizing process of the related parameters [23].

In this research, experiment design, statistical data analysis using Stat-Ease Design-Expert software (version 11), response surface method as a mathematical and statistical tool to optimize variables affecting adsorption such as solution pH, adsorbent amount, the initial concentration of the drug, contact time and temperature for the adsorption of the cefixime drug were performed as the response (output). Table 1 shows different experimental levels of independent factors and their codes. Table 1 basically consists of 2^n factorials and $2 \times n$ axial paths along with the number of central points (p). Eq. 1 is used to calculate the number of test runs based on the number of input variables:

$$N_p = [2^m + (2 \times m) + p] \quad (1)$$

where Np indicates the number of necessary test executions, m indicates the number of variables affecting the output of the process. In this research, the value of m is equal to 5.

Table 1. Different levels for independent parameters affecting drug absorption

code	independent parameters	unit	-1	0	+1
A	pH	-	4	7	10
B	Absorbent dose	g	0.01	0.03	0.05
C	Drug concentration	ppm	10	30	50
D	Temperature	℃	30	50	70
E	Contact time	min	20	35	50

The central composite design consists of 3 steps, which include starting the experiment design, calculating the model coefficients, predicting the model's behavior, and calculating the results [24]. The experiments lead to the creation of an empirical model that calculates the functional behavior based on the input parameters along with their related combinations, and a second-order polynomial model is obtained for the analysis and prediction of drug loading as shown in Eq. 2:

$$Y = \beta_0 + \sum_{i=1}^{5} \beta_i X_i + \sum \beta_{ij} X_i X_j \quad (2)$$

where Y and (X_i and X_j) respectively represent the response of drug absorption in terms of percentage and coded independent factors. β_0 is a constant value, while β_i, β_{ii}, and β_{ij} represent the linear, quadratic, and interactive

coefficients of the input independent variables, respectively [25]. A total of 50 runs by the response surface model were proposed by the software to investigate the effects of five independent factors on drug absorption as presented in Table S1.

Results and Discussions

Characterization of mesostructure of SBA-16-NH_2

The FTIR spectrum of SBA-16 and SBA-16-NH_2 can be seen in Fig 4a. As shown in Figure 4a, a broad peak at 3441.12 cm^{-1} is associated with the symmetric stretching vibration of the O-H bond of the Si-OH silanol groups. Also, the peak observed at 1630.95 cm^{-1} is associated with the stretching and bending vibrations of the water molecules adsorbed on the SBA-16 surface. The peaks at 463.52 cm^{-1}, 805.2 cm^{-1} and 1086.21 cm^{-1} are associated with the symmetric and asymmetric Si-O-Si bending, stretching and bending vibrations, respectively. The above data confirm that the synthesized material is a silicate mesoporous [26]. The observed band at 1085.30 cm^{-1} is related to the asymmetric stretching vibrations of Si-O-Si and around 797.37 cm^{-1} and 949.10 cm^{-1} is dedicated to the symmetric stretching vibrations of the Si-O-Si bond. Also, the bands observed in the region of 471.94 cm^{-1} represent tetrahedral silica due to the presence of SiO_4 units. The broad band of 16.3414 cm^{-1} refers to the O-H stretching vibration mode of silanol groups. Bands assigned to C-H stretching vibrations of propyl chains were observed around 2930 cm^{-1} in the spectrum of the sample containing amine. (C-H)ν and (C-H)δ deformation vibrations in methyl groups were observed in the regions of 1463.39 cm^{-1} and 1353 cm^{-1} in the spectrum of the sample containing amine [27]. Also, in the XRD analysis related to mesopore SBA-16 and SBA-16-NH_2 (Fig 4b), a very strong peak at 2θ = 20-30°. corresponding to the (110) plane, and the next three weak peaks at a higher angle, corresponding to the (211) plane, are observed. This issue confirms the presence of a cubic structure of space group Im3m [28]. Fig 4c shows the scanning electron microscope (SEM) image of the surface of the synthesized SBA-16 and SBA-16-NH_2 samples. According to this micrograph, it can be concluded that the synthesized samples of SBA-16 and SBA-16-NH_2 has spherical and homogeneous morphology. Also, the size of the pores is in the range of 2-50 nm, which proves that the synthesized material is a mesoporous one [29]. TEM image taken of the SBA-16-NH_2 mesostructure at a magnification of 100 nm is shown in Fig. 4d. This image shows a highly ordered cage-like arrangement of mesopores. Figure 4e shows the adsorption-desorption isotherm diagram of SBA-16-NH_2. As can be seen, this nanocomposite has a type IV isotherm and the adsorption curve does not coincide with the desorption curve and forms a ring called hysteresis. When a compound forms a hysteresis ring in its isotherm diagram, it can be said that the compound has 100% mesopores. Also, by using the adsorption-desorption isotherm diagram and the hysteresis ring formed, the geometry of the pores can be identified. According to the diagram, the hysteresis ring is of type H1. Therefore, the pores have a cylindrical geometry [30]. Table 2 shows the results of BET analysis of mesoporous SBA-16-NH_2. The results indicate that the specific surface area of SBA-16-NH_2 is 258.64 m^2/g. Also, the average particle diameter and pore volume were 4.098 nm and 0.5876 cm^3/g, respectively. Therefore, it can be concluded that the synthesized SBA-16-NH_2 is mesoporous. The thermal stability of the samples was determined by thermogravimetric analysis (Fig 4f). The mass loss between room temperature and 200°C corresponds to the release of absorbed moisture. It should be noted that mass loss in this temperature range is reduced as a result of modification with amine groups. At the higher temperatures, thermal decomposition of the amine ligands took place and the decomposition was completed at 800°C. For samples modified with amine groups, only one main peak was observed at 400 ℃ [31].

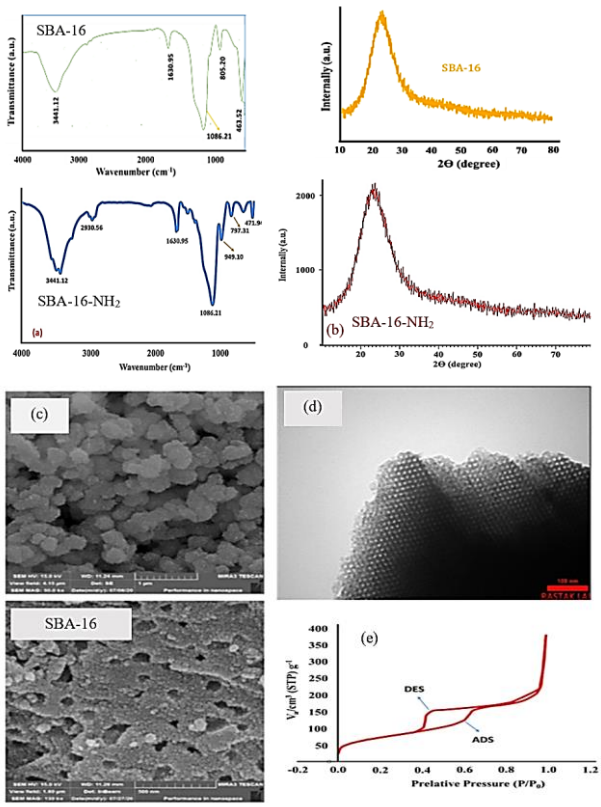

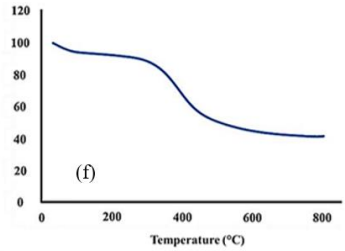

Fig 4. (a) FTIR spectrum, (b) XRD analysis, (c) SEM image, (d) TEM image (e) N_2 adsorption-desorption isotherm (f) TGA analysis

Table 2. BET analysis results

BET table		
V_m	59.423	[cm^3(STP) g^{-1}]
$a_{s,BET}$	258.64	[m^2 g^{-1}]
C	174.6	
Total pore volume(p/p_0=0.988)	0.5876	[cm^3 g^{-1}]
Average pore diameter	4.087	[nm]

Statistical analysis

After the tests, the results were given to the software to provide the best model for evaluating and describing the data. The proposed model of the software was among the four linear, interactive, quadratic and cubic models, the quadratic model was the most consistent with the responses. It happened because the best and most suitable model is determined based on the p-value values and regression coefficients [32 As can be seen in Table 3, the quadratic model has a p-value less than 0.05 and the highest regression coefficient compared to the other 3 models.

Table 3. The results related to the statistical analysis of cefixime drug removal on SBA-16-NH_2 nanoadsorbent

Source	Seq. p-value	Lack of Fit p-value	Adj. R^2	Pred. R^2	
Linear	< 0.0001	< 0.0001	0.8717	0.8532	
2FI	0.0750	< 0.0001	0.8941	0.8670	
Quadratic	< 0.0001	0.5826	0.9967	0.9940	Suggested
Cubic	0.5820	0.4935	0.9966	0.9705	Aliased

The results of the analysis of variance (ANOVA) for drug removal are shown in Table 4, where a P-value less than 0.05 indicates that the model terms are significant and a higher F-value indicates a more significant effect of the model terms. Statistically, a small p-value and a large F-value indicate the importance of a model or a parameter [33]. As shown in Table 4, according to the high F-value (748.72) and very low p-value (p<0.0001), the quadratic model is highly significant for the removal of cefixime antibiotic [34]

Table 4. Results of ANOVA analysis of variance of removal of cefixime antibiotic on SBA-16-NH_2 nanoadsorbent

Source	Sum of Squares	df	Mean Square	F-value	p-value	
Model	12377.64	20	618.88	748.72	< 0.0001	Sig.
A	16.84	1	16.84	20.38	< 0.0001	
B	248.62	1	248.62	300.77	< 0.0001	
C	10614.72	1	10614.72	12841.59	< 0.0001	
D	71.34	1	71.34	86.31	< 0.0001	
E	21.17	1	21.17	25.61	< 0.0001	
AB	7.32	1	7.32	8.86	0.0058	
AC	10.05	1	10.05	12.15	0.0016	
AD	4.11	1	4.11	4.97	0.0336	
AE	1.57	1	1.57	1.90	0.1786	
BC	426.69	1	426.69	516.20	< 0.0001	
BD	0.2683	1	0.2683	0.3246	0.5733	
BE	5.69	1	5.69	6.88	0.0137	
CD	7.19	1	7.19	8.70	0.0062	
CE	7.42	1	7.42	8.98	0.0056	
DE	47.17	1	47.17	57.06	< 0.0001	
A^2	2.58	1	2.58	3.12	0.0879	
B^2	60.75	1	60.75	73.50	< 0.0001	
C^2	155.58	1	155.58	188.22	< 0.0001	
D^2	0.1788	1	0.1788	0.2163	0.6454	
E^2	62.30	1	62.30	75.37	< 0.0001	
Res.	23.97	29	0.8266			
Lack of Fit	17.90	22	0.8137	0.9386	0.5826	not sig.
Pure Error	6.07	7	0.8669			
Cor Total	12401.61	49				

The appropriateness of the equation of the proposed model (polynomial) was checked with the help of R^2, R^2 Adj. and R^2 Pred. A high value of R^2 indicates a better fit of the equation with the experimental data. According to Table 5, the values of predicted R^2 and adjusted R^2 are 0.9940 and 0.9967, respectively. The closer these values are to one, more adequately confirm the quadratic model for more drug loading. Also, the sum of squares of R or R^2 is equal to 0.9981. This number means that 99.81% of the response variable changes can be explained using the proposed software model [35].

Table 5. Regression coefficients of the quadratic model

Std. Dev.	0.9092	R^2	0.9981
Mean	70.12	Adjusted R^2	0.9967
C.V. %	1.30	Predicted R^2	0.9940
		Adeq Precision	84.8709

Confirmation of the experimental results can be obtained by analyzing the graphics obtained from the response surface model by model accuracy graphs including experimental vs. predicted values, standard residual

values vs. predicted values, and standard residual values vs. experimental values. The high agreement between the experimental and predicted values of the high percentage of drug removal by SBA-16-NH_2 nanoadsorbent is shown in Fig 5a. According to the figure, the experimental values of the drug removal efficiency and the predicted values have a high degree of agreement. From Fig 5a, it can be inferred that the predicted points and the experimental results are closer to each other [36]. These observations show that the experimental results for this research are very acceptable. Fig 5b and c show the standardized residuals against the experimental and predicted values, confirming that the observed errors are normally distributed with a confidence interval of ±3.67. According to Fig 5b, it can be seen that the points are scattered around the horizontal line, which indicates that there is no significant change between the actual and predicted [37].

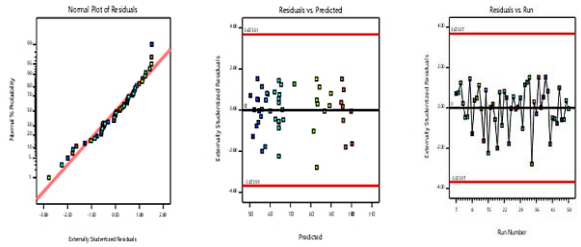

(a) (b) (c)

Fig 5. (a). Predicted values vs. experimental values, (b). Standard balance vs. predicted values, (c). Standard vs. experimental values

The effect of parameters on the rate of cefixime antibiotic removal

Determination of pH is one of the most important aspects in drug removal at different pH levels. At a pH lower than pH_{zpc}, due to the high concentration of H^+ ions in the environment, the surface charge of the adsorbent is positive [38]. Therefore, positively charged adsorbents can effectively absorb negatively charged drug molecules. But at pH higher than pH_{pzc}, due to the high concentration of OH^- ions, the surface charge of the adsorbent becomes negative. As a result, the repulsion created between the positively charged adsorbent and the negatively charged drug molecules reduces the amount of drug removal. Experiments were performed for cefixime drug removal efficiency in the pH range between 4 and 10. The results are shown in Fig 6a. In acidic conditions, the removal efficiency of cefixime antibiotic increased and decreased in alkaline conditions. The highest rate of cefixime antibiotic removal on SBA-16-NH_2 was obtained at pH = 4. The increase in removal of cefixime antibiotic in acidic conditions is related to the electrostatic attraction force of cefixime drug with SBA-16-NH_2. At lower pH (pH = 4), the increase in electrostatic attraction between cefixime drug and SBA-16-NH_2 surface leads to the increase of cefixime removal.

Fig 6b shows the effect of adsorbent dose on the absorption of cefixime drug by SBA-16-NH_2 nanoadsorbent. The removal percentage increases with the increase of dose up to 0.049 g. The increase in the removal percentage is due to the increase in the active sites of the adsorbent. However, with a further increase in the adsorbent dose, the removal percentage is quite constant, because at a higher adsorbent dose, the concentration of cefixime molecules in the solution is not enough to cover all the adsorption sites on the adsorbent surface. Therefore, the equilibrium adsorbent dose for cefixime drug was 0.049 g and this value was used for subsequent experiments [39].

The effect of the initial concentration of cefixime on absorption efficiency was investigated in the range of drug concentration 10-50 mg/liter. The present study shows that the nanoadsorbent can absorb up to 10 mg/L of drug. The effect of the initial drug concentration factor is determined by the interaction between the binding sites on the adsorbent surface and the drug concentration. In most conditions, the proportion of drug removed decreases with increasing initial drug concentration. This can be due to the saturation of the adsorbent surface with adsorption sites. When the drug concentration is low, there are empty active sites on the adsorbent surface. But, as the concentration increases, the active sites required for drug absorption are not available. In other words, as the initial concentration of the drug increases, the remaining concentration of the drug molecules will be higher. While at lower concentrations, the ratio of the initial number of drug molecules to unoccupied adsorption sites is minimal. Fig 6c shows the effect of initial drug concentration (10 mg/L) [40].

Cefixime drug adsorption on SBA-16-NH_2 nano-absorbent was investigated in the temperature range of 30, 50 and 70 ℃ (Fig 6d). The results showed that the amount of drug removal decreases with increasing temperature. The decrease in removal can be attributed to changes in Gibbs free energy. As the temperature increases, the enthalpy and entropy changes become negative, and according to the thermodynamic relationship $\Delta G = \Delta H - T\Delta S$, the entropy becomes positive, as a result, the Gibbs free energy becomes positive. Therefore, at low temperatures, the absorption process is spontaneous [41].

The relationship between cefixime removal and contact time is shown in Fig 6f. This figure indicates

that the time required to reach equilibrium adsorption is directly proportional to the removal. The experiments showed that in the first 35 minutes, from 0 to 35 minutes, the removal of cefixime increased rapidly due to the large amount of surface area of mesoporous particles available

for removal. Then, from 35 to 50 minutes, cefixime drug removal decreased with time, and this was due to the decrease in the availability of mesoporous particle surface for removal. However, the drug adsorption graph became almost horizontal after 50 minutes, indicating that the surfaces of the mesoporous particles were filled (saturated) or, in other words, reached the equilibrium absorption level. The best loading time was the first 35 minutes [42].

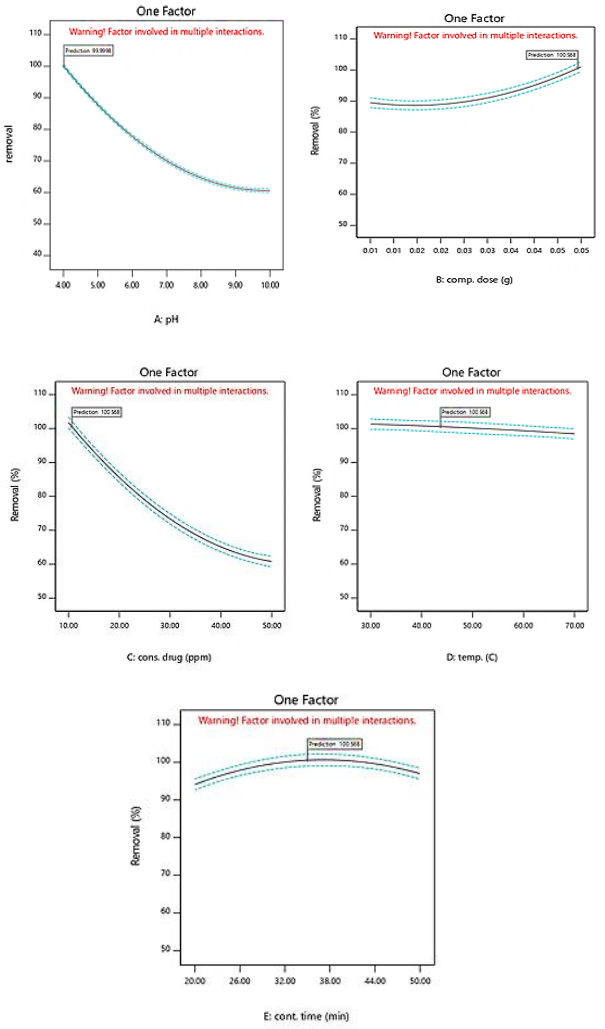

Fig 6. Effect of independent parameters on the amount of drug removal, (a). effect of pH, (b). effect of nanoadsorbent dosage, (c). effect of drug concentration, (d). effect of temperature, (f). effect of contact time

Interaction effects of independent variables

The interaction effects of dependent variables on drug adsorption are presented in Fig 7. According to Fig 7a, drug adsorption increases with increasing adsorbent dose from 0.01 to 0.05 g/L and decreasing pH from 10 to 4. When other parameters were kept constant, the maximum drug removal was at pH = 4 and dose. The adsorbent was 0.049 g and the optimum pH for drug adsorption was 4. In Fig 7b, when the initial drug concentration increases from 10 to 50 mg/L, the drug removal rate decreases in all adsorbent doses. However, the interaction between drug removal concentration and adsorbent dose was statistically insignificant, especially at low adsorbent doses. Fig 7c shows the interaction between pH and drug concentration. As can be seen in this figure, while the pH and initial drug concentration decrease, the drug removal increases. Therefore, the interaction effect of pH and drug concentration is significant. The decrease in drug removal with increasing initial drug concentration can be attributed to the fact that with increasing drug concentration, the number of active sites on the adsorbent surface is not enough to absorb all the drug molecules, so drug removal decreases [43, 44].

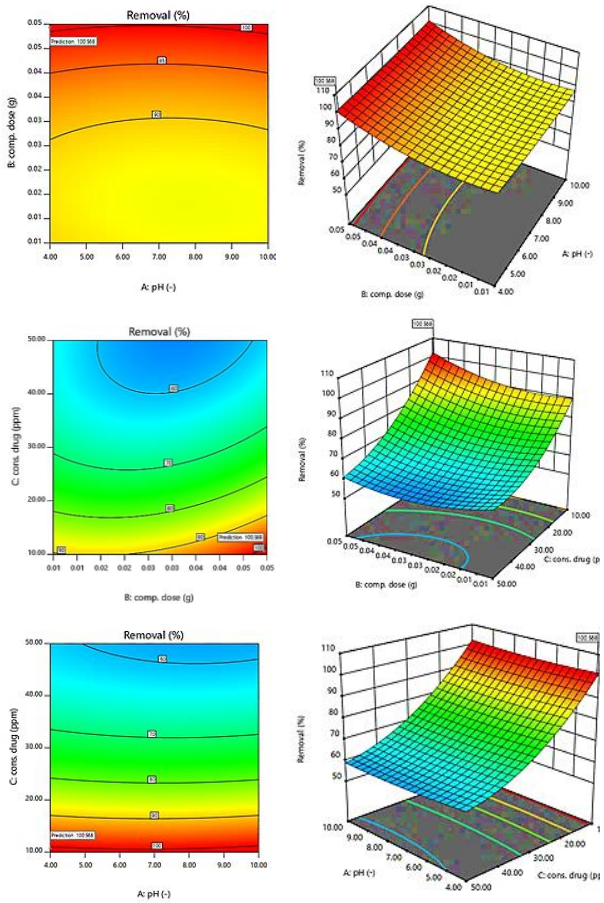

Fig 7. The mutual effect of independent parameters on the rate of cefixime antibiotic removal

Optimization studies

To evaluate the optimal conditions for the maximum adsorption of cefixime drug, five pH variables, amount of nanosorbent, initial drug concentration, temperature and contact time were studied in the range suggested by the software. Experiment design software, pH = 4, nanoadsorbent dose 0.049 g, drug concentration 10 mg/L,

temperature 43 ℃ and contact time 35 min as optimal conditions to achieve maximum absorption of cefixime antibiotic 99.99 % with the desirability of 1 suggested. The experiments were repeated under the predicted optimal conditions. The results are reported in Table 6, where the experimental data were very close to the predicted value, confirms the validity and adequacy of the model.

Table 6. The optimal values of independent variables for maximum absorption of cefixime drug

parametr	pH	Ads. dose	drug cons.	Temp.	Cont. time	Removal %	
						Real	Pred.
Opt. value	4.00	0.049	10.00	43.00	35.00	98.88	99.99

Adsorption isotherm

The adsorption isotherm determines the transfer of the adsorbed material to the adsorbent in equilibrium conditions. Interactions between drug and adsorbent molecules and maximum adsorption capacity can be described by equilibrium isotherms. Therefore, Langmuir, Freundlich and Temkin models were studied to describe the adsorption of cefixime on SBA-16-NH_2 adsorbent (Fig 8). Adsorption isotherm experiments were performed under optimal conditions and different drug concentrations of 10, 30 and 50 mg/L.

Langmuir isotherm describes the monolayer and homogeneous adsorption of drug molecules on the adsorbent surface [45]. The linear form of the Langmuir isotherm is expressed as Eq. 3
:

$$\frac{1}{q_e} = \frac{1}{q_m} + \left(\frac{1}{q_m K_L}\right)\frac{1}{C_e} \quad (3)$$

where q_e (mg/g), C_e (mg/L), q_{max} (mg/g) and K_L(l/mg) and respectively the amounts of absorbed drug in the equilibrium state, the equilibrium concentration of the absorbed substance, the maximum absorption capacity and are Langmuir equilibrium constants. K_L and q_{max} values are calculated from the graph of $1/C_e$ versus $1/q_e$ [46].

The Freundlich isotherm assumes that drug adsorption on a heterogeneous adsorbent surface is multilayered. The linear form of the Freundlich isotherm is as described in Eq. 4:

$$\log q_e = \log k_F + \frac{1}{n}\log C_e \quad (4)$$

where n (l/mg) and K_F (mg/g) are the Freundlich constant and absorption intensity, respectively. K_F and n can be determined from the linear plot of log q_e versus log C_e [47].

Temkin isotherm is used for adsorbents in which the active sites of adsorption are not the same in terms of energy and chemical adsorption that is carried out in the form of a single layer. The linear form of Temkin isotherm is defined based on Eq. 5
:

$$q_e = B_1 \ln C_e + \ln K_T \quad (5)$$

K_T is the Temkin isotherm constant and B_1 depends on the heat of the surface adsorption process. The values of B_1 and $\ln K_T$ are calculated by drawing the graph of $\ln C_e$ against q_e and determining the equation of the line using the slope and width of the origin [48].
The isotherm parameters for the adsorption of cefixime antibiotic on SBA-16-NH_2 adsorbent are given in Table 7, where the highest correlation coefficient of 1 corresponds to the Langmuir isotherm, which shows that the adsorption data are well fitted with the Langmuir isotherm.

Table 7. Isotherm parameters for absorption of cefixime antibiotic on SBA-16-NH_2 nanosorbent

Parameter	Adsorption isotherm
Langmuir	
q_{max} (mg.g^{-1})	35.71
K_L (l/mg)	1.94
R^2	1.00
Freundlish	
n	3.66
K_F ($mg^{-1(1/n)}L^{1/n}g^{-1}$)	17.65
R^2	0.8616
Temkin	
B	5.3754
K_T (l/mg)	1.34
R^2	0.9139

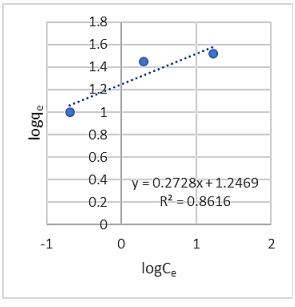

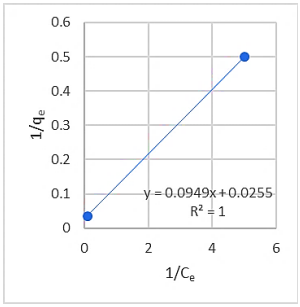

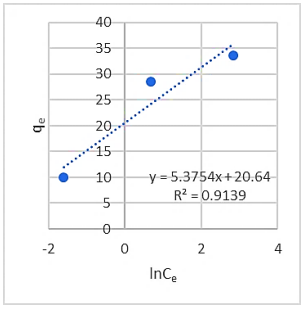

Fig 8. Langmuir isotherm, Freundlich isotherm and Temkin isotherm of absorption of cefixime antibiotic on SBA-16-NH_2 nanoadsorbent

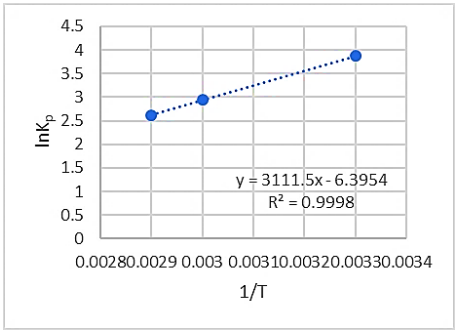

Fig 9. Thermodynamic diagram of cefixime antibiotic adsorption on SBA-16-NH_2 nanoadsorbent

Table 8. Values of thermodynamic parameters of drug adsorption

Temp. (K)	lnK	ΔH° ($Kj.mol^{-1}$)	ΔS° ($Kj.mol^{-1}$)	ΔG° ($Kj.mol^{-1}$)	R^2
303	3.87			-9.27	
333	2.95	-25.86	-0.053	-8.21	0.9998
343	2.62			-7.68	

Adsorption thermodynamics

Thermodynamic studies are necessary to evaluate whether the adsorption process is spontaneous or not. It also helps to identify whether the absorption process is endothermic or exothermic. Adsorption thermodynamics at different temperatures were studied to estimate the effect of temperature on the drug absorption process [49]. Various thermodynamic parameters, such as enthalpy changes (ΔH^o), entropy changes (ΔS^o), and Gibbs free energy changes (ΔG^o), can be evaluated from Equations 6 to 9.

$$K = \frac{q_e}{C_e} \quad (6)$$

$$\Delta G^\circ = -RT\ln K \quad (7)$$

$$\Delta G^\circ = \Delta H^\circ - T\Delta S^\circ \quad (8)$$

$$\ln K = \frac{\Delta H^\circ}{RT} + \frac{\Delta S^\circ}{R} \quad (9)$$

where, K represents the equilibrium constant, T is the adsorption temperature (K) and R represents the universal gas constant (8.314 J/mol.K). Using the slope and width from the origin of the 1/T diagram, the value of ΔH^o and ΔS^o is obtained in terms of lnK.

According to Fig 9, the negative value of enthalpy showed that the absorption process of cefixime drug on SBA-16-NH_2 adsorbent is exothermic. The amount of entropy also decreases in the absorption process due to the location of the absorbed molecules on the absorbent surface as a result of their regularization, the negative sign of entropy is also for this reason. The negative values obtained for Gibbs free energy indicate the spontaneity of the absorption process of cefixime drug by SBA-16-NH_2 adsorbent, according to the obtained results, the value of ΔG^o increases with decreasing temperature, which is based on eq 8 and with considering the negative values of entropy and enthalpy, the reduction of Gibbs free energy is not far from expected [50].

Adsorption kinetics

Fast reaction speed, short contact time and significant adsorption capacity are the necessary conditions for an effective adsorption process. To better clarify the characteristics of the adsorption process, three kinetic models, pseudo first order, pseudo second order and Higuchi kinetics were used in optimal conditions to describe the change of the effective number of active sites on the surface of the adsorbent during adsorption (Fig 10).

The pseudo-first order model is expressed as Eq. 10:

$$\ln(q_e - q_t) = -k_1 t - lnq_e \quad (10)$$

where q_e (mg/g) and q_t (mg/g) are adsorption capacity at the moment of equilibrium and time t. k_1 (min^{-1}) and t (min) are the reaction rate and time constants, respectively. K_1 and qe are calculated from the linear graph of ln ($q_e - q_t$) versus time, respectively [51].

The pseudo-second order model is expressed by Eq. 11:

$$\frac{t}{q_t} = \frac{1}{k_2 q_e^2} + \frac{1}{q_e} t \quad (11)$$

Where k_2 (g/mg min) is the pseudo-second order rate constant. q_e and k_2 are determined from the slope and width from the origin of the linear graph of t/q_t against t [52].

Kinetics of Higuchi model assumes that the intraparticle diffusion of drug molecules on the adsorbent is the rate-limiting step in the absorption process [53]. The Higuchi kinetics model is expressed as Eq. 12:

$$q_t = k_{id}\sqrt{t} + C \quad (12)$$

The kinetic parameters for the removal of cefixime antibiotic by SBA-16-NH_2 nanoadsorbent are given in Table 9. The correlation coefficients in this table show that the absorption data follow the pseudo first order model (R^2 = 0.9997).

Table 9. Kinetic parameters for the adsorption of the antibiotic cefixime on SBA-16-NH_2 nanoadsorbent

Parameter	Kinetic model
pseudo first order	
q_e (mg.g^{-1})	39.18
k_1 (min^{-1})	-0.011
R^2	0.9997
pseudo-second order	
q_e (mg.g^{-1})	90.9
k_2 (mg.g^{-1}.min^{-1})	0.000046
R^2	0.9852
Higuchi model	
C (mg.g^{-1})	2.6182
k_{id} (mg.g^{-1}.min$^{-1/2}$)	0.1126
R^2	0.9766

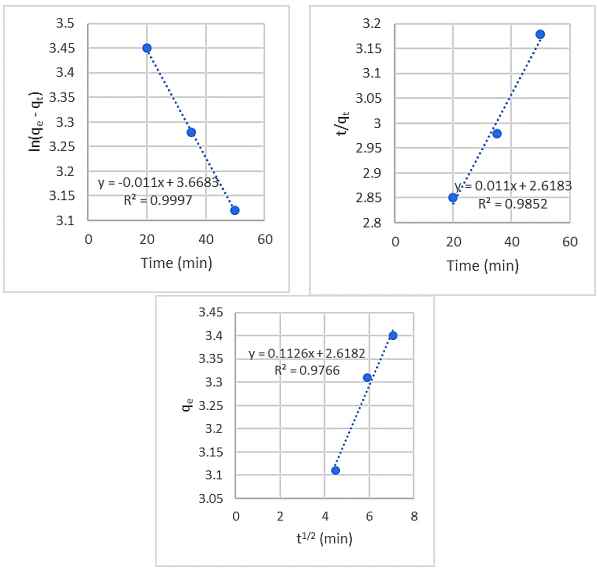

Fig 10. pseudo-first-order, pseudo-second-order, and intraparticle kinetics of cefixime drug adsorption

Conclusions

In this research, silicate mesoporous SBA-16-NH_2 was synthesized by sol-gel method and its use as an adsorbent for the removal of cefixime antibiotic from aqueous solutions was investigated. The results of XRD analysis showed that SBA-16-NH_2 was synthesized with a cubic network with a very good structural order. Parameters affecting drug removal including pH, nanoadsorbent dose, drug concentration, temperature, and contact time were optimized using response surface method experiment design software. The software suggested the optimal values for pH = 4, nanosorbent dose 0.049 g, drug concentration 10 mg/L, temperature 43 ℃ and contact time 35 min to achieve the maximum amount of drug removal (98.88%). The isotherm studies carried out among the three isotherms of Langmuir, Freundlich and Temkin showed that the adsorption process of cefixime is highly consistent with the Langmuir isotherm. Based on thermodynamic studies, the adsorption of cefixime drug by SBA-16-NH_2 nanoadsorbent is a spontaneous process. Examining the rate of adsorption by three pseudo-first-order kinetics, pseudo-second-order kinetics and Higuchi model showed that the adsorption of cefixime drug by nanoadsorbent is compatible and consistent with the pseudo first order model. According to the obtained results, mesoporous SBA-16-NH_2 can be used as an ideal adsorbent to remove the pharmaceutical pollutant cefixime from aqueous environments.

Acknowledgements

The authors express their appreciation to post-graduate office of Lorestan and Farhangian University for financial support of this work.

References

[1] Velempini, T., Prabakaran, E., Pillay, K., Recent developments in the use of metal oxides for photocatalytic degradation of pharmaceutical pollutants in water-a review, ***Materials Today Chemistry*, 2021,** *19*, 100380. https://doi.org/10.1016/j.mtchem.2020.100380.

[2] Bustos Bustos, E., Sandoval-González, A., Martínez-Sánchez, C., Detection and treatment of persistent pollutants in water: general review of pharmaceutical products, ***ChemElectroChem*, 2022,** *9*(12), e202200188. https://doi.org/10.1002/celc.202200188.

[3] Nava-Andrade, K., Carbajal-Arízaga, G. G., Obregón, S., Rodríguez-González, V., Layered double hydroxides

and related hybrid materials for removal of pharmaceutical pollutants from water, ***Journal of Environmental Management*, 2021,** 288, 112399. https://doi.org/10.1016/j.jenvman.2021.112399.

[4] González-González, R. B., Sharma, A., Parra-Saldívar, R., Ramirez-Mendoza, R. A., Bilal, M., Iqbal, H. M., Decontamination of emerging pharmaceutical pollutants using carbon-dots as robust materials, ***Journal of Hazardous Materials*, 2022,** 423, 127145. DOI: 10.1016/j.jhazmat.2021.127145.

[5] Taoufik, N., Boumya, W., Janani, F. Z., Elhalil, A., Mahjoubi, F. Z., Removal of emerging pharmaceutical pollutants: a systematic mapping study review, ***Journal of Environmental Chemical Engineering*, 2020,** 8(5), 104251. https://doi.org/10.1016/j.jece.2020.104251.

[6] Issaka, E., Amu-Darko, J. N. O., Yakubu, S., Fapohunda, F. O., Ali, N., Bilal, M., Advanced catalytic ozonation for degradation of pharmaceutical pollutants-A review, ***Chemosphere*, 2022,** 289, 133208. DOI: 10.1016/j.chemosphere.2021.133208.

[7] Renita, A. A., Sathish, S., Kumar, P. S., Prabu, D., Manikandan, N., Iqbal, A. M., Rangasamy, G., Emerging aspects of metal ions-doped zinc oxide photocatalysts in degradation of organic dyes and pharmaceutical pollutants–A review, ***Journal of Environmental Management*, 2023,** 344, 118614. DOI: 10.1016/j.jenvman.2023.118614 .

[8] Sahay, P., Mohite, D., Arya, S., Dalmia, K., Khan, Z., Kumar, A., Removal of the emergent pollutants (hormones and antibiotics) from wastewater using different kinds of biosorbent-a review, ***Emergent Materials*, 2023,** 6(2), 373-404. DOI: 10.1007/s42247-023-00460-9**.**

[9] Muteeb, G., Rehman, M. T., Shahwan, M., Aatif, M., Origin of antibiotics and antibiotic resistance, and their impacts on drug development: A narrative review, ***Pharmaceuticals*, 2023,** 16(11), 1615. DOI: 10.3390/ph16111615.

[10] Caneschi, A., Bardhi, A., Barbarossa, A., Zaghini, A., The use of antibiotics and antimicrobial resistance in veterinary medicine, a complex phenomenon: A narrative review, ***Antibiotics*, 2023,** 12(3), 487. DOI: 10.3390/antibiotics12030487.

[11] Anuar, N. F., Shah, D. R. S. I., Ramli, F. F., Zaini, M. S. M., Mohammadi, N. A., Daud, A. R. M., Syed-Hassan, S. S. A., The removal of antibiotics in water by chemically modified carbonaceous adsorbents from biomass: A systematic review, ***Journal of Cleaner Production*, 2023,** 401, 136725. DOI:10.1016/j.jclepro.2023.136725.

[12] Mangla, D., Sharma, A., & Ikram, S., Critical review on adsorptive removal of antibiotics: Present situation, challenges and future perspective, ***Journal of Hazardous Materials*, 2022,** 425, 127946. DOI: 10.1016/j.jhazmat.2021.127946.

[13] Baaloudj, O., Nasrallah, N., Bouallouche, R., Kenfoud, H., Khezami, L., Assadi, A. A., High efficient Cefixime removal from water by the sillenite $Bi_{12}TiO_{20}$: Photocatalytic mechanism and degradation pathway, ***Journal of Cleaner Production*, 2022,** 330, 129934. DOI:10.1016/j.jclepro.2021.129934.

[14] Patel, S., Sharma, J., Gole, V. L., Removal of antibiotic cefixime from wastewater using UVC/Sodium persulphate system, ***Materials Today: Proceedings*, 2023,** 78, 69-73. https://doi.org/10.3390/w15101819.

[15] Ortúzar, M., Esterhuizen, M., Olicón-Hernández, D. R., González-López, J., Aranda, E., Pharmaceutical pollution in aquatic environments: a concise review of environmental impacts and bioremediation systems, ***Frontiers in microbiology*, 2022,** 13, 869332. DOI: 10.3389/fmicb.2022.869332.

[16] Arman, N. Z., Salmiati, S., Aris, A., Salim, M. R., Nazifa, T. H., Muhamad, M. S., Marpongahtun, M., A review on emerging pollutants in the water environment: Existences, health effects and treatment processes, ***Water*, 2021,** 13(22), 3258. https://doi.org/10.3390/w13223258.

[17] Porrang, S., Davaran, S., Rahemi, N., Allahyari, S., & Mostafavi, E., How advancing are mesoporous silica nanoparticles? A comprehensive review of the literature, ***International Journal of Nanomedicine*, 2022,** 1803-1827. DOI: 10.2147/IJN.S353349.

[18] Pal, N., Lee, J. H., Cho, E. B., Recent trends in morphology-controlled synthesis and application of mesoporous silica nanoparticles, ***Nanomaterials*, 2020,** 10(11), 2122. https://doi.org/10.3390/nano10112122.

[19] Tsai, Cheng-Hsun, et al. "Functionalization of cubic mesoporous silica SBA-16 with carboxylic acid via one-pot synthesis route for effective removal of cationic dyes. ***Journal of hazardous materials*, 2016,** 309, 236-248. https://doi.org/10.1016/j.jhazmat.2015.08.051.

[20] Sayadi, K., Rahdar, A., Hajinezhad, M. R., Nikazar, S., Susan, M. A. B. H., Atorvastatin-loaded SBA-16 nanostructures: Synthesis, physical characterization, and biochemical alterations in hyperlipidemic rats, ***Journal of Molecular Structure*, 2020,** 1202, 127296. DOI:10.1016/j.molstruc.2019.127296.

[21] Soleymani, S., Razavi Mehr, M., Fekri, M. H., Saki, F., Modification of SBA-16 surface by-NH_2 group and its application as adsorbent, ***Chemical Papers*, 2023,** 77(9), 5129-5141. DOI: 10.1007/s11696-023-02849-6.

[22] Sarkar, S., Tiwari, N., Behera, M., Chakrabortty, S., Jhingran, K., Sanjay, K., Tripathy, S. K., Facile synthesis, characterization and application of magnetic Fe_3O_4-coir pith composites for the removal of methyl violet from aqueous solution: Kinetics, isotherm, thermodynamics and parametric optimization, ***Journal of the Indian Chemical Society*, 2022,** 99(5), 100447. DOI:10.1016/j.jics.2022.100447.

[23] Ghorbani, F., Kamari, S., Core–shell magnetic nanocomposite of Fe_3O_4@ SiO_2@ NH_2 as an efficient and highly recyclable adsorbent of methyl red dye from aqueous environments, ***Environmental Technology & Innovation*, 2019,** 14, 100333. DOI:10.1016/j.eti.2019.100333.

[24] Bagherlou, N., Ghasemi, E., Gharbani, P., Babazadeh, M., Mehrizad, A., Optimization and modeling of betamethasone removal from aqueous solutions using a SiO_2/g-C_3N_5@$NiFe_2O_4$ nanophotocatalyst by RSM, ***npj Clean Water*, 2024,** 7(1), 2. DOI:10.1038/s41545-023-00295-1.

[25] Mahmoudi, S., Otadi, M., Hekmati, M., Monajjemi, M., Shekarabi, A. S., Methylene blue removal from aqueous solution using modified Met-SWCNT-Ag nanoparticles: optimization using RSM-CCD, ***International Journal of Chemical Reactor Engineering*, 2023,** 21(10), 1177-1197. https://doi.org/10.1515/ijcre-2022-0240.

[26] Sayadi, K., Rahdar, A., Hajinezhad, M. R., Nikazar, S., & Susan, M. A. B. H. Atorvastatin-loaded SBA-16 nanostructures: Synthesis, physical characterization, and biochemical alterations in hyperlipidemic rats. ***Journal of Molecular Structure*, 2020,** *1202*, 127296. https://doi.org/10.1016/j.molstruc.2019.127296

[27] Naghiloo, M., et al. "Functionalization of SBA-16 silica particles for ibuprofen delivery. ***Journal of Sol-Gel Science and Technology*, 2015,** 74, 537-543. https://doi.org/10.1007/s10971-015-3631-6.

[28] Goscianska, J., Olejnik, A., Nowak, I., APTES-functionalized mesoporous silica as a vehicle for antipyrine–adsorption and release studies, ***Colloids and Surfaces A: Physicochemical and Engineering Aspects*, 2017,** 533, 187-196. https://doi.org/10.1016/j.colsurfa.2017.07.043.

[29] Bhuyan, D., Saikia, M., Saikia, L., Magnetically recoverable Fe_3O_4@SBA-15: An improved catalyst for three component coupling reaction of aldehyde, amine and alkyne, ***Catalysis Communications*, 2015,** 58, 158-163. DOI:10.1016/j.catcom.2014.09.011.

[30] Ezzeddine, Z., Batonneau-Gener, I., & Pouilloux, Y. Zinc removal from water via EDTA-modified mesoporous SBA-16 and SBA-15. ***Toxics*,** *2023*, 11(3), 205. https://doi.org/10.3390/toxics11030205

[31] Feliczak-Guzik, A., Jadach, B., Piotrowska, H., Murias, M., Lulek, J., Nowak, I., Synthesis and characterization of SBA-16 type mesoporous materials containing amine groups. ***Microporous and Mesoporous Materials*, 2016,** 220, 231-238. https://doi.org/10.1016/j.micromeso.2015.09.006.

[32] Fekri, M. H., Soleymani, S., Mehr, M. R., Akbari-adergani, B., Synthesis and characterization of mesoporous ZnO/SBA-16 nanocomposite: Its efficiency as drug delivery system, ***Journal of Non-Crystalline Solids*, 2022,** 591, 121512. DOI:10.1016/j.jnoncrysol.2022.121512.

[33] Dalvand, A., Nabizadeh, R., Ganjali, M. R., Khoobi, M., Nazmara, S., Mahvi, A. H., Modeling of Reactive Blue 19 azo dye removal from colored textile wastewater using L-arginine-functionalized Fe_3O_4 nanoparticles: Optimization, reusability, kinetic and equilibrium studies, ***Journal of Magnetism and Magnetic Materials*, 2016,** 404, 179-189. https://doi.org/10.1016/j.jmmm.2015.12.040.

[34] Reghioua, A., Barkat, D., Jawad, A. H., Abdulhameed, A. S., Al-Kahtani, A. A., & ALOthman, Z. A., Parametric optimization by Box–Behnken design for synthesis of magnetic chitosan-benzil/ZnO/Fe_3O_4 nanocomposite and textile dye removal, ***Journal of Environmental Chemical Engineering*, 2021,** 9(3), 105166. DOI:10.1016/j.jece.2021.105166.

[35] Mirzaei, A., Yerushalmi, L., Chen, Z., Haghighat, F., Photocatalytic degradation of sulfamethoxazole by hierarchical magnetic ZnO@ g-C_3N_4: RSM optimization,

kinetic study, reaction pathway and toxicity evaluation, ***Journal of hazardous materials*, 2018,** 359, 516-526.
DOI: 10.1016/j.jhazmat.2018.07.077.

[36] Jaswir, I., Noviendri, D., Taher, M., Mohamed, F., Octavianti, F., Lestari, W., Hamad Almansori, B. B., Optimization and formulation of fucoxanthin-loaded microsphere (F-LM) using response surface methodology (RSM) and analysis of its fucoxanthin release profile, ***Molecules*, 2019,** 24(5), 947.
DOI: 10.3390/molecules24050947.

[37] Zhang, X., Zhou, J., Xu, Y., Optimized parameters for the preparation of silk fibroin drug-loaded microspheres based on the response surface method and a genetic algorithm–backpropagation neural network model, ***Journal of Biomedical Materials Research Part B: Applied Biomaterials*, 2021,** 109(1), 6-18.
https://doi.org/10.1002/jbm.b.34676.

[38] Afrashteh, S., Nouri, N., Banihashem, P., Hoseinpour Kasgari, A., Valipour, P., Binaeian, E., Methotrexate drug uptake through dimethyl ethylenediamine post-modified metal–organic framework as a carrier: optimization using RSM, ***Journal of Porous Materials*, 2023,** 1-17.
DOI:10.1007/s10934-023-01441-3.

[39] Nazari zadeh, E., Fozooni, S., Tavakkoli Nejad, E., Khaleghi, M., Synthesis of Fe_3O_4@MCM41 and Kaolinite Coated with Ethyl 2-((3-(Triethoxysilyl) Propylamino) (Phenyl) methyl)-3-Oxobutanoate and their Applications in Heavy Metal Removal and Drug Delivery: Optimization Study Using RSM. *Silicon*, 1-28.
DOI:10.1007/s12633-023-02341-6.

[40] Matei, D., Katsina, A. U., Mihai, S., Cursaru, D. L., Șomoghi, R., & Nistor, C. L. (2023). Synthesis of ruthenium-promoted ZnO/SBA-15 composites for enhanced photocatalytic degradation of methylene blue dye, ***Polymers*, 2023,** 15(5), 1210.
https://doi.org/10.3390/polym15051210.

[41] Fekri, M. H., Saki, F., Razavi-mehr, M., Soleymani, S., Preparation of SBA-16 silicate nanoabsorbent by green method from reed plant stem, using it to remove Phenolphthalein pollutant and investigating effective factors by RSM method, ***Applied Chemistry*, 2023,** 9-26.
DOI: 10.22075/chem.2023.29594.2141.

[42] Fard, N. T., Panahi, H. A., Banadaki, M. D., Moniri, E., Soltani, E. R., Surface Modification of Graphene Oxide by Functionalized Dendritic Polyesters Based on Phthalic Acid and Pentaerythritol as a Novel Nanoplatform for Sustained Drug Delivery: Statistical Optimization using Response Surface Methodology and Release Kinetics Modelling, ***Materials Today Communications*, 2023,** 106476.
DOI:10.1016/j.mtcomm.2023.106476.

[43] Mohammed, B. B., Hsini, A., Abdellaoui, Y., Abou Oualid, H., Laabd, M., El Ouardi, M., Tijani, N., Fe-ZSM-5 zeolite for efficient removal of basic Fuchsin dye from aqueous solutions: Synthesis, characterization and adsorption process optimization using BBD-RSM modeling, ***Journal of Environmental Chemical Engineering*, 2020,** 8(5), 104419.
DOI:10.1016/j.jece.2020.104419.

[44] Kang, J. K., Kim, Y. G., Lee, S. C., Jang, H. Y., Yoo, S. H., Kim, S. B., Artificial neural network and response surface methodology modeling for diclofenac removal by quaternized mesoporous silica SBA-15 in aqueous solutions, ***Microporous and Mesoporous Materials*, 2021,** 328, 111497.
https://doi.org/10.1016/j.micromeso.2021.111497·

[45] Al-Ghouti, M. A., Da'ana, D. A., Guidelines for the use and interpretation of adsorption isotherm models: A review, ***Journal of hazardous materials*, 2020,** 393, 122383.
https://doi.org/10.1016/j.jhazmat.2020.122383.

[46] Majd, M. M., Kordzadeh-Kermani, V., Ghalandari, V., Askari, A., Sillanpää, M., Adsorption isotherm models: A comprehensive and systematic review (2010−2020), ***Science of The Total Environment*, 2022,** 812, 151334.
DOI: 10.1016/j.scitotenv.2021.151334.

[47] Wang, J., Guo, X., Adsorption isotherm models: Classification, physical meaning, application and solving method, ***Chemosphere*, 2020,** 258, 127279.
https://doi.org/10.1016/j.chemosphere.2020.127279.

[48] Alsuhaibani, A. M., Alayyafi, A. A., Albedair, L. A., El-Desouky, M. G., El-Bindary, A. A., Efficient fabrication of a composite sponge for Cr (VI) removal via citric acid cross-linking of metal-organic framework and chitosan: adsorption isotherm, kinetic studies, and optimization using Box-Behnken design, ***Materials Today Sustainability*, 2024,** 26, 100732.
https://doi.org/10.1016/j.mtsust.2024.100732.

[49] Lima, E. C., Hosseini-Bandegharaei, A., Moreno-Piraján, J. C., Anastopoulos, I., A critical review of the estimation of the thermodynamic parameters on adsorption equilibria. Wrong use of equilibrium constant in the Van't Hoof equation for calculation of thermodynamic parameters of adsorption, ***Journal of molecular liquids*, 2019,** 273, 425-434.
https://doi.org/10.1016/j.molliq.2018.10.048.

[50] Osagie, C., Othmani, A., Ghosh, S., Malloum, A., Esfahani, Z. K., Ahmadi, S., Dyes adsorption from aqueous media through the nanotechnology: A review, ***Journal of Materials Research and Technology*****, 2021,** 14, 2195-2218.
DOI:10.1016/j.jmrt.2021.07.085.

[51] Wang, J., & Guo, X., Adsorption kinetic models: Physical meanings, applications, and solving methods, ***Journal of Hazardous materials*****, 2020,** 390, 122156.
https://doi.org/10.1016/j.jhazmat.2020.122156.

[52] Revellame, E. D., Fortela, D. L., Sharp, W., Hernandez, R., Zappi, M. E., Adsorption kinetic modeling using pseudo-first order and pseudo-second order rate laws: A review, ***Cleaner Engineering and Technology*****, 2020,** 1, 100032.
https://doi.org/10.1016/j.clet.2020.100032.

[53] Hubbe, M. A., Azizian, S., Douven, S., Implications of apparent pseudo-second-order ads orption kinetics onto cellulosic materials: A review, ***BioResources*****, 2019,** 14(3).
DOI: 10.15376/biores.14.3.7582-7626.